Power Spectral Analysis of UW-OFDM Systems

Morteza Rajabzadeh, *Member, IEEE*, and Heidi Steendam, *Senior Member, IEEE*

***Abstract*— Unique word- (UW-) orthogonal frequency division multiplexing (OFDM) is a new multicarrier technique that is shown to be superior to the cyclic prefix- (CP-) OFDM system in terms of bit-error-rate performance in fading channels. Furthermore, in the literature, it is shown by simulations that UW-OFDM has a considerably lower out-of-band (OOB) radiation compared with CP-OFDM. In this paper, we derive an analytical expression to investigate the spectral characteristics of UW-OFDM to be able to determine the effect of the different system parameters on the OOB radiation. In addition, we include in our analysis the effects of the interpolation filter and the unique word. We show that the OOB radiation in UW-OFDM is mainly determined by the number of non-modulated subcarriers reserved as the guard band, and the ratio of the UW sequence length to the number of subcarriers. By increasing either of these two parameters, we show that we can suppress the OOB radiation to any amount. This is an important advantage of UW-OFDM over classic CP-OFDM systems, and shows that UW-OFDM is an excellent candidate for cognitive radio systems.**

***Index Terms*— Power spectral density, UW-OFDM, out-of-band radiation.**

I. Introduction

OVER the past decades, multicarrier systems have attracted significant interest in the research community, and since they can achieve flexible high data rates while being robust against frequency selective channels and still have a simple receiver, they were adopted in many wired and wireless standards. In multicarrier systems, the data is transmitted block-wise, where in each block the data symbols are modulated by an inverse discrete Fourier transform (IDFT). To avoid intersymbol interference, the blocks are separated by a guard interval. In the most widespread type of multicarrier systems, i.e. CP-OFDM, the output of the IDFT is extended by adding a cyclic prefix as a guard interval. Zero padding (ZP) [1], known symbol padding (KSP) [2] and time domain synchronous padding (TDS) [3] are other methods to fill the guard interval. Common to these techniques is that they all extend the symbol length: the duration of a symbol is the IDFT length plus the guard interval length. In a recently proposed multicarrier technique, i.e. UW-OFDM, the guard interval is part of the IDFT block. Hence, the duration of a symbol equals the IDFT length, irrespective of the guard interval length. This guard interval is filled with a known and deterministic sequence, which is repeated every IDFT block. As such, similarly as in the traditional multicarrier techniques (CP-, ZP-, KSP- and TDS-OFDM), the linear convolution, resulting from the data sequence passing through the channel, transforms to a circular convolution, which simplifies channel equalization. Moreover, in contrast to the cyclic prefix in CP-OFDM, which is a random sequence as it depends on the random data symbols, but similarly to KSP- and TDS-OFDM, the content of the guard interval is prior known to the receiver, implying it can be designed for particular transmission purposes like synchronization or channel estimation. Because in UW-OFDM, part of the time-domain block must be fixed, the sequence that is modulated on the carriers must contain redundancy. Depending on how the redundancy is added, two types of UW-OFDM can be distinguished. In systematic UW-OFDM, the redundancy is located on a selected set of subcarriers, i.e. the data carriers and redundant carriers belong to disjoint subsets [4], whereas, in non-systematic UW-OFDM, the redundancy is spread over all the active subcarriers [5].

Until now, different performance metrics of UW-OFDM have already been analyzed in the literature. In [6], the spectrum efficiency of UW-OFDM is studied for different transmission settings, and it is shown that for similar communication settings UW-OFDM and CP-OFDM have essentially the same data throughput: the required addition of redundancy in the frequency domain in UW-OFDM is compensated by the reduction of the block length compared to CP-OFDM. Further, to fully exploit the available redundancy, more sophisticated detectors are required for UW-OFDM. In contrast, in CP-OFDM, a simple linear data estimator is sufficient. Multiple (linear and non-linear) data estimators were derived for UW-OFDM [5], [7]–[11], and the overhead complexity of the different data detectors was studied in [10]. Although the complexity of the data estimator is higher than for CP-OFDM, it is shown that for the same bandwidth efficiency [5] or the same theoretical achievable data rate [7], UW-OFDM outperforms CP-OFDM in fading channels, in terms of the bit error rate performance, which is the result of the diversity gain introduced in the UW-OFDM data structure [12]. Although this diversity gain comes at the cost of an additional data detection complexity, the difference in complexity will diminish when additional channel coding such as turbo coding is used, as the (turbo) decoder has much higher complexity than the data detector.

Manuscript received September 12, 2016; revised March 4, 2017 and May 19, 2017; accepted July 4, 2017. Date of publication July 17, 2017; date of current version June 14, 2018. This research has been funded by the Interuniversity Attraction Poles Programme initiated by the Belgian Science Policy Office. The associate editor coordinating the review of this paper and approving it for publication was J. Choi. *(Corresponding author: Morteza Rajabzadeh.)*

M. Rajabzadeh is with the Electrical Engineering Department, Quchan University of Technology, Quchan, Khorasan Razavi, Iran (e-mail: m.rajabzadeh@qiet.ac.ir).

H. Steendam is with the Department of Telecommunications and Information Processing, Ghent University, 9000 Gent, Belgium (e-mail: heidi.steendam@ugent.be).

Color versions of one or more of the figures in this paper are available online at http://ieeexplore.ieee.org.

Digital Object Identifier 10.1109/TCOMM.2017.2728058

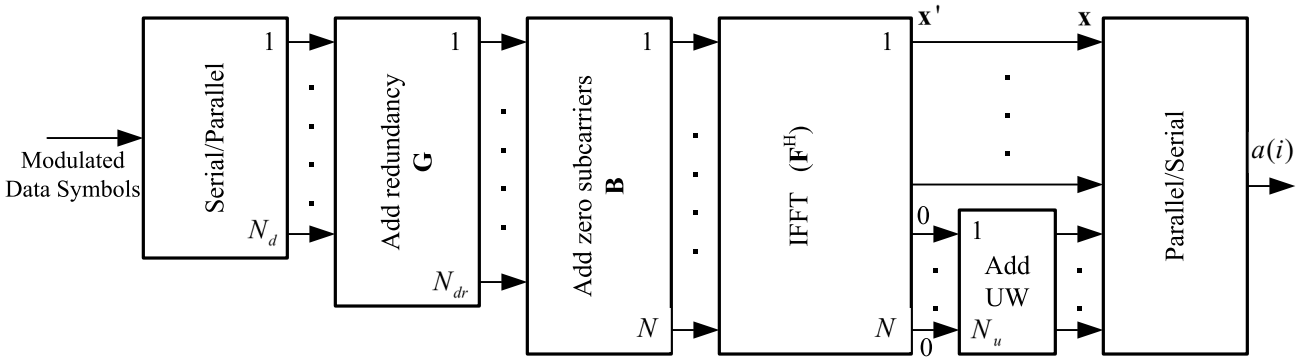

Fig. 1. Block diagram of a typical UW-OFDM transmitter.

In communication systems that have to meet spectral regulatory masks, such as cognitive radio, the spectral behavior is an important performance metric. In such a case, it is important to be able to control the in-band and out-of-band (OOB) radiation of the system. To our best knowledge, the spectral behavior of UW-OFDM is only considered in [5], where the authors claim that UW-OFDM has lower OOB radiation than CP-OFDM. These results are based on simulations only, which does not offer deep insight in how to control the spectrum, and do not consider the effect of the interpolation filter and the presence of the unique word. Therefore, considering the fact that UW-OFDM has shown promising results in terms of BER, throughput efficiency and OOB radiation, in this paper, we address the power spectrum characterization of UW-OFDM to obtain a more in-depth understanding of the good spectral behavior of UW-OFDM. The effects of different UW-OFDM parameters on the power spectral density (PSD) and OOB radiation are studied both analytically and through simulations. We derive analytical expressions for the PSD of both UW-OFDM system types - systematic and non-systematic coded UW-OFDM. These expressions will pave the road to easily control the OOB radiation of the UW-OFDM system. In this paper, we show that we can reduce the OOB radiation as well as the roll-off factor of the UW-OFDM spectrum by increasing either the number of guard band subcarriers, or the ratio of the UW length to the number of subcarriers. It turns out that we can suppress the OOB radiation to a level that is 160 dB lower than the level of the in-band containing the useful signal. Taking into account the numerical precision of the computations, this implies that we can reduce the OOB radiation to essentially zero, even if no interpolation filter is used. Further, we investigate the effect of the interpolation filter. This paper is an extension to our previous work on the spectral behavior of UW-OFDM [13], which only considered the case of systematic UW-OFDM. Not only this paper generalizes the results to non-systematic UW-OFDM systems, but also it studies the effect of different UW-OFDM parameters on the OOB radiation of UW-OFDM system, and considers the effect of the addition of the unique word on the spectrum. It turns out that when the UW contains a standard sequence, as e.g. a constant amplitude, zero autocorrelation (CAZAC) sequence which is employed for channel estimation and synchronization, the good OOB radiation property of UW-OFDM is destroyed. To solve this problem, we propose a novel construction method for the unique word, resulting in good OOB radiation properties. It is noteworthy that filterbank multicarrier and OFDM/OQAM schemes are other types of multicarrier techniques which provide good OOB radiation properties [14], [15]. However, considering the implementation issues, they belong to another family of MC techniques that need more complex transmitters/receivers. On the other hand, UW-OFDM provides the good OOB radiation property with the same transceiver structure as CP-OFDM, which is based on the IFFT/FFT.

Taking into account the excellent OOB radiation and spectral shaping properties of UW-OFDM, it can be used in systems complying with strict spectrum regulatory masks. Specifically, UW-OFDM is an excellent candidate for cognitive radio systems that are designed to use the spectrum holes in the spectrum without imposing considerable interference on adjacent bands used by the primary system.

The paper structure is as follows. After the introduction, in Section II, the system models of systematic and non-systematic coded UW-OFDM are described. Also, we introduce a novel approach to build the code generator matrix for non-systematic coded UW-OFDM, which provides a more structured framework for analyzing and developing non-systematic coded UW-OFDM compared to the iterative method proposed in [5]. In Section III, the analytical expressions for the PSD of both types of UW-OFDM systems are derived, and the effects of the interpolation filter and the unique word sequence are highlighted. Section IV describes the simulation results, analyzes different aspects of the UW-OFDM spectrum and compares the PSD of UW-OFDM with that of conventional CP-OFDM.

II. System Model

The block diagram of a typical UW-OFDM transmitter is shown in Fig. 1. Let $\tilde{\mathbf{d}} \in \mathbb{C}^{N_d \times 1}$ be the vector of N_d modulated data symbols that are independently and identically distributed ($E\{\tilde{\mathbf{d}}\tilde{\mathbf{d}}^H\} = \sigma^2 \mathbf{I}_{N_d}$) with zero mean ($E\{\tilde{\mathbf{d}}\} = \mathbf{0}_{N_d \times 1}$). Without loss of generality, we assume $\sigma^2 = 1$. The UW-OFDM signal is constructed by first generating N_u zeros at the output of the N-point IDFT block. This is

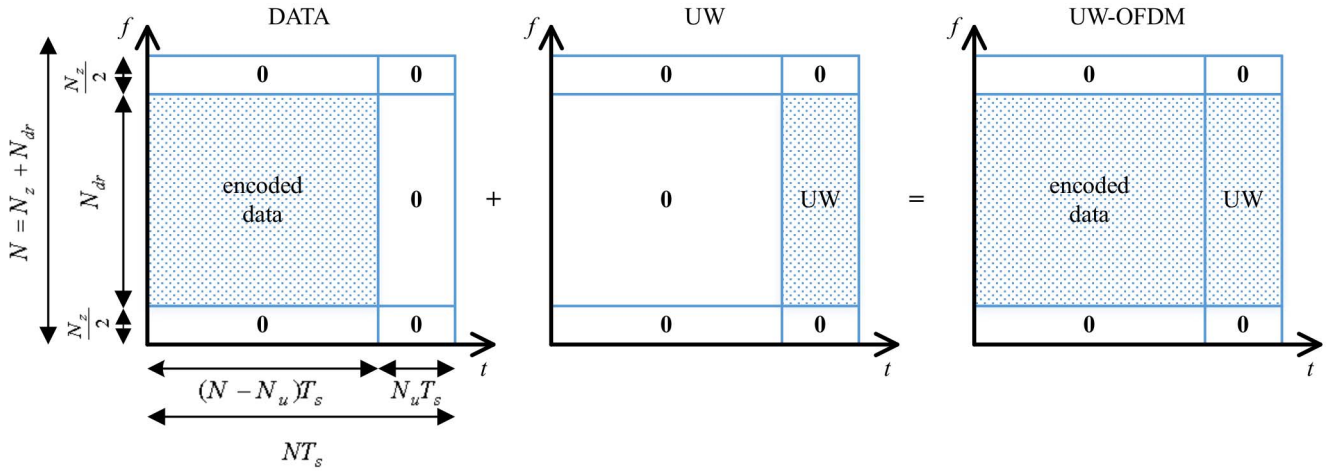

Fig. 2. The time-frequency structure of UW-OFDM with N_z zero carriers at the band edges and a unique word with length $N_u T_s$, where T_s is the sample duration.

done by adding redundancy in the frequency domain by using a precoder matrix, $\mathbf{G} \in \mathbb{C}^{N_{dr} \times N_d}$, where $N_{dr} = N_d + N_r$, i.e. N_r is the amount of redundancy that is introduced, with $N_r \geq N_u$. As this construction resembles a Reed-Solomon code (in the complex field), the precoding matrix is also called the code generator matrix. Like in standard multicarrier systems, $N_z = (N - N_{dr})$ zero subcarriers are placed, e.g. at band edge and DC subcarriers.[1] The data vector at the frequency domain is given by

$$\tilde{\mathbf{x}} = \mathbf{B}\mathbf{G}\tilde{\mathbf{d}}, \tag{1}$$

where $\mathbf{B} \in \mathbb{R}^{N \times N_{dr}}$ adds the zero subcarriers, i.e. the columns of $\mathbf{B}$ are unit vectors. The precoder is selected to generate a block of N_u zeros at the end of the output of the IDFT block. Hence, before adding the unique word, the $N \times 1$ time-domain data vector is given as

$$\mathbf{x}' = \mathbf{F}_N^H \mathbf{B}\mathbf{G}\tilde{\mathbf{d}} = \begin{bmatrix} \mathbf{x}_d \\ \mathbf{0}_{N_u \times 1} \end{bmatrix}, \tag{2}$$

where $\mathbf{F}_N^H$ is the $N \times N$ IDFT matrix, and $\mathbf{x}_d$ is the $(N - N_u) \times 1$ time-domain vector that depends on the transmitted data symbols, $\tilde{\mathbf{d}}$. After replacing the zeros by the desired unique word, $\mathbf{x}_u \in \mathbb{C}^{N_u \times 1}$, the time-domain data vector is obtained as

$$\mathbf{x} = \mathbf{x}' + \begin{bmatrix} \mathbf{0}_{(N-N_u)\times 1} \\ \mathbf{x}_u \end{bmatrix} = \begin{bmatrix} \mathbf{x}_d \\ \mathbf{x}_u \end{bmatrix}. \tag{3}$$

The time-frequency structure of the UW-OFDM data block is shown in Fig. 2, for which a guard band containing N_z zero subcarriers is considered at the band edges. Depending on how the redundancy is added, we can distinguish two types of UW-OFDM: systematic coded UW-OFDM and non-systematic coded UW-OFDM [5].

A. Systematic Coded UW-OFDM

In this approach, N_r subcarriers are dedicated to sending the redundant data. This is done by defining the matrix $\mathbf{G}$ as

$$\mathbf{G} = \mathbf{P}\begin{bmatrix} \mathbf{I}_{N_d} \\ \mathbf{T} \end{bmatrix}, \tag{4}$$

[1]Note that the set of N_z zero subcarriers can also include guard bands required to avoid interference to primary users in a cognitive radio system.

where $\mathbf{P} \in \mathbb{R}^{N_{dr} \times N_{dr}}$ is a permutation matrix determining the places of the data and redundant subcarriers, and $\mathbf{T} \in \mathbb{C}^{N_r \times N_d}$ is a transform matrix creating the redundant symbols, $\tilde{\mathbf{r}} = \mathbf{T}\tilde{\mathbf{d}} \in \mathbb{C}^{N_r \times 1}$, based on the data vector $\tilde{\mathbf{d}}$. The data vector at time domain can be expressed as

$$\mathbf{x}' = \mathbf{F}_N^H \mathbf{B}\mathbf{P}\begin{bmatrix} \mathbf{I} \\ \mathbf{T} \end{bmatrix}\tilde{\mathbf{d}} = \mathbf{F}_N^H \mathbf{B}\mathbf{P}\begin{bmatrix} \tilde{\mathbf{d}} \\ \tilde{\mathbf{r}} \end{bmatrix}. \tag{5}$$

Let us define a new matrix as follows:

$$\mathbf{M} = \mathbf{Q}\mathbf{P} = \begin{bmatrix} \mathbf{M}_1 & \mathbf{M}_2 \end{bmatrix}, \tag{6}$$

where $\mathbf{Q}$ is the $N_u \times N_{dr}$ matrix built by the N_u lowermost rows of $\mathbf{F}_N^H \mathbf{B}$, $\mathbf{M}_1 \in \mathbb{C}^{N_u \times N_d}$ and $\mathbf{M}_2 \in \mathbb{C}^{N_u \times N_r}$. To obtain the block of N_u zeros in the time-domain, we have to impose the following restriction: $\mathbf{M}_1\tilde{\mathbf{d}} + \mathbf{M}_2\tilde{\mathbf{r}} = \mathbf{0}$. This is fulfilled by choosing $\mathbf{T} = \mathbf{M}_2^{\dagger}\mathbf{M}_1$, where $\mathbf{M}_2^{\dagger} = \mathbf{M}_2^H(\mathbf{M}_2\mathbf{M}_2^H)^{-1}$ is the Moore-Penrose pseudo-inverse. The problem in systematic coded UW-OFDM is the rather high energy that has to be spent on the redundant symbols [16], [17].

B. Non-Systematic Coded UW-OFDM

The problem of the high energy requirement of systematic coded UW-OFDM is solved in [5] by spreading the redundancy on all subcarriers. This is done by designing an appropriate non-systematic code generator matrix, $\mathbf{G} \in \mathbb{C}^{N_{dr} \times N_d}$. So, on top of creating the required zeros at the output of the IDFT, the code generator matrix is designed to distribute the redundant energy on all subcarriers. Compared to the systematic coded UW-OFDM implementation, the original data symbols, $\tilde{\mathbf{d}}$, do not appear directly on the subcarriers after being multiplied with $\mathbf{G}$. Therefore, this implementation of UW-OFDM systems is called non-systematic coded UW-OFDM, which is comparable to a non-systematic code defined over the field of complex numbers. Typically, it is assumed that the transmitted power per data symbol is normalized; this requires $trace\{\mathbf{G}^H\mathbf{G}\} = N_d$. Huemer *et al.* [5] suggest to select the code generator matrix $\mathbf{G}$ to minimize the error covariance of a best linear unbiased estimator (BLUE) and a linear minimum mean square error (LMMSE) data estimator

at the receiver. They show that the optimum $\mathbf{G}$ should satisfy $\mathbf{G}^H\mathbf{G} = \mathbf{I}$. However, the proposed iterative method to calculate the optimum $\mathbf{G}$ is not suitable for analyzing the different performance aspects of the UW-OFDM system. Therefore, we consider the decomposition of the generator matrix, $\mathbf{G}$, proposed in [12] and [18] as

$$\mathbf{G} = \mathbf{N}_Q\mathbf{C}, \tag{7}$$

where $\mathbf{N}_Q = Null(\mathbf{Q}) \in \mathbb{C}^{N_{dr}\times(N_{dr}-N_u)}$ is the matrix containing the $N_{dr}-N_u$ orthonormal null space vectors of $\mathbf{Q}$ (defined in (6)), and the $(N_{dr}-N_u)\times N_d$ matrix $\mathbf{C}$ can be selected freely. Optimization of the generator matrix in many situations only involves the optimization of $\mathbf{C}$, as the matrix $\mathbf{N}_Q$ is fixed and determined by the system parameters, i.e. the number and positions of the zero subcarriers, the UW length, amount of added redundancy and the DFT size. In the following, we restrict our attention to the case where $\mathbf{C}^H\mathbf{C} = \mathbf{I}$, as this corresponds to the minimization of the BLUE or LMMSE data estimators [5].

III. Power Spectral Density of the UW-OFDM System

In conventional CP-OFDM, several theoretical methods to derive the PSD are available. The method that is most commonly used, is based on the analog implementation of the multicarrier system, and is employed, e.g. for spectrum modeling [19], blind carrier tracking [20], in-band and OOB radiation reduction and sidelobe suppression [21]–[23]. However, although this analytical model is easy to use, the model is not precise for practical systems, where the multicarrier transmitter is implemented by an IDFT followed by a digital-to-analog converter (DAC) [24].

To find a more precise model for the PSD of a multicarrier system, we revert to the definition of the PSD. Let us consider a sequence of symbols $a[i]$, which is passed through a DAC. The analog signal at the output is given as

$$s(t) = \sum_{i=-\infty}^{+\infty} a\,[i]\,g_I(t - iT_s), \tag{8}$$

where T_s is the sample duration, and $g_I(t)$ is the impulse response of the interpolation filter. In the case the discrete-time sequence $a[i]$ is stationary with autocorrelation function (ACF) $R(i;m) = R(m) \triangleq E\{a^*[i]a[i+m]\}$, the PSD of the digital-to-analog converted signal is given as

$$P(f) = \frac{|G_I(f)|^2}{T_s}P_x(f), \tag{9}$$

where $G_I(f)$ is the Fourier transform of $g_I(t)$, and $P_x(f) = \mathcal{F}[R(m)]$ is the Fourier transform of the autocorrelation function $R(m)$.

In multicarrier systems, the above expression for the PSD cannot be used straightforward, as the discrete-time sequence $a[i]$ is not stationary. However, when the transmitted data bits are i.i.d.. and the same transmitter structure is used for every multicarrier block (e.g. same number of modulated carriers with fixed guard bands), the sequence at the output of the DAC is cyclostationary. Taking into account that the data symbols in the different multicarrier blocks are statistically independent, it was proposed in [1] and [25] to obtain the average $P_x(f)$ by time-averaging the ACF upon one cyclic period and replace it in (9). van Waterschoot *et al.* [1] have found an approximate analytical expression for the PSD of CP-OFDM and ZP-OFDM, by further presuming that the frequency-domain symbols modulated on the subcarriers are i.i.d. However, because of the redundancy added in the frequency domain, the frequency-domain symbols modulated on the different subcarriers are not uncorrelated in UW-OFDM. Hence, the method of [1] and [25] cannot be used to find closed-form expressions for the PSD of UW-OFDM.

In order to derive precise closed-form expressions for the PSD in UW-OFDM, we employ the principle of the Periodogram method, which is used to estimate the PSD of an observed data sequence. In this method, the PSD is calculated as the squared magnitude of the Fourier transform of the available samples. As in practice the estimation variance of the Periodogram method is high, a variant to reduce this variance is proposed by Bartlett [26]. In Bartlett's method, the available samples are split into shorter data segments, and the PSD is estimated as the time-averaged Fourier transform of the data in the segments. We now translate Bartlett's method to estimate the PSD from a sequence of observed samples into a theoretical method to derive an approximate closed-form expression for the PSD for UW-OFDM. Taking into account that the UW-OFDM signal is random and cyclostationary, we replace the time average in Bartlett's method by a statistical average. In Appendix A, we show that we can select the length of the data segments to a UW-OFDM block length because (i) the data symbols in the different UW-OFDM blocks are statistically independent, and (ii) the data correlation pattern in the successive UW-OFDM blocks is repeated. This can be understood by considering the block-based representation of the analog signal in (8):

$$s(t) = \sum_{l=-\infty}^{+\infty}\sum_{n=0}^{N-1} x_n^{(l)} g_I(t - (lN+n)T_s), \tag{10}$$

where $x_n^{(l)} = a[lN+n]$. As a consequence, the PSD of the discrete-time sequence, $a[i]$, in (8) is approximated as

$$P_x(f) = E\left[\left|X^{(l)}(f)\right|^2\right], \tag{11}$$

where $X^{(l)}(f)$ is the discrete-time Fourier transform (DTFT) [27] of the lth UW-OFDM block ($\mathbf{x}^{(l)} = \left[x_0^{(l)}, x_1^{(l)}, \ldots, x_{N-1}^{(l)}\right]^T$), and is given as

$$X^{(l)}(f) = \frac{1}{\sqrt{N}}\sum_{n=0}^{N-1} x_n^{(l)} e^{-jn2\pi f T_s}. \tag{12}$$

The PSD of the analog baseband signal, $s(t)$ in (10), is finally obtained by substituting (11) in (9).

In this paper, two terms are used to point to the entire frequency band: in-band and out-of-band (OOB). Assuming the time-domain symbol rate is T_s, the spectrum, $P_x(f)$, is periodic with period $1/T_s$. Throughout the paper, we will consider the equivalent baseband frequency band, so that the

spectra will be shown at two sides of the zero frequency, i.e. we will consider the interval $[-1/T_s, 1/T_s]$. In this regard, we define the in-band as the part of the mentioned frequency interval, $[-1/T_s, 1/T_s]$, where the subcarriers are not nulled. The out-of-band (OOB) is defined to be the part of the interval $[-1/T_s, 1/T_s]$ corresponding to the nulled (guard) subcarriers at both sides of the in-band, and also covers all other frequencies outside the mentioned frequency interval. Considering the above definition, equation (9) comprises of two parts. The first part, $|G_I(f)|^2$, is the interpolation filter frequency response with cut-off frequency $1/2T_s$. This should be designed to be flat in spectrum in-band, and to have a sharp spectral roll-off such that OOB radiation of the system to be rapidly suppressed. The second part, $P_x(f)$, solely relates to the characteristics of the transmitted data and unique word, and determines both the in-band and the OOB spectral behavior of the UW-OFDM system. Based on (11)-(12), one can observe that $P_x(f)$ is periodic with a period $1/T_s$. So, the interpolation filter should reject the excessive OOB parts of the UW-OFDM spectrum resulting from the signal periodicity.

Let us look closer at the PSD (11) of the discrete-time sequence $\mathbf{x}^{(l)}$. Using vector notation, the DTFT values in (12) can be written as $X^{(l)}(f) = \mathbf{e}(f)\mathbf{x}^{(l)}$, where $\mathbf{e}(f)$ is a $1 \times N$ row vector with nth entry as $e^{-jn2\pi fT_s}/\sqrt{N}$. From (3), it follows that the time-domain data vector contains the contributions of the data and the unique word. In practice, the unique word is a deterministic and known sequence, which is repeated in each UW-OFDM block. Further, the transmitted data symbols are statistically independent of the unique word contribution, and have zero mean. Therefore, the PSD (11) can be decomposed into a contribution from the data and the unique word:

$$P_x(f) = P_{x,d}(f) + P_{x,u}(f), \tag{13}$$

where the contribution from the deterministic unique word $\mathbf{x}_u$ is given by

$$P_{x,u}(f) = \mathbf{e}(f)\begin{bmatrix}\mathbf{0} & \mathbf{0}\\ \mathbf{0} & \mathbf{x}_u\mathbf{x}_u^H\end{bmatrix}\mathbf{e}^H(f), \tag{14}$$

and the contribution from the random data symbols $P_{x,d}(f)$ depends on the statistical properties of the transmitted data only, and is given as

$$\begin{aligned} P_{x,d}(f) &= E\left\{\mathbf{e}(f)\mathbf{x}'^{(l)}\mathbf{x}'^{(l)^H}\mathbf{e}^H(f)\right\}\\ &= \mathbf{e}(f)\mathbf{F}_N^H\mathbf{B}\mathbf{G}\mathbf{G}^H\mathbf{B}^H\mathbf{F}_N\mathbf{e}^H(f)\\ &= trace\left\{\mathbf{G}^H\mathbf{B}^H\mathbf{F}_N\mathbf{e}^H(f)\mathbf{e}(f)\mathbf{F}_N^H\mathbf{B}\mathbf{G}\right\} \end{aligned} \tag{15}$$

where we have used (2). Let us look closer at the expression (15). The product $\mathbf{e}(f)\mathbf{F}_N^H$ is given by

$$\left\{\mathbf{e}(f)\mathbf{F}_N^H\right\}_k = \frac{1}{N}\frac{1-e^{-j2\pi N(k/N-fT_s)}}{1-e^{-j2\pi(k/N-fT_s)}}.$$

Note that when $f = m/NT_s$, the above expression reduces to $\left\{\mathbf{e}(m/NT_s)\mathbf{F}_N^H\right\}_k = \delta_{k,m}$, implying the product $\mathbf{F}_N\mathbf{e}^H(f)\mathbf{e}(f)\mathbf{F}_N^H$ is a diagonal matrix where the mth diagonal element is a one, and all other diagonal elements are zero. Further, $\mathbf{B}$ is a column-reduced identity matrix determining which carriers are modulated. Hence, at frequency $f = m/NT_s$, $P_{x,d}(f)$ reduces to the energy of the symbol transmitted on carrier m, i.e. $\left\{\mathbf{B}\mathbf{G}\mathbf{G}^H\mathbf{B}^H\right\}_{m,m}$, which equals zero for a non-modulated carrier.

A. PSD of Systematic Coded UW-OFDM

To obtain the PSD for the special case of a systematic coded UW-OFDM transmission, it is sufficient to substitute the code generator matrix given in (4) into the above relations. Hence, before the D/A conversion, the PSD is given by:

$$P_x(f) = \mathbf{e}(f)\mathbf{F}_N^H\mathbf{B}\mathbf{P}\begin{bmatrix}\mathbf{I} & \mathbf{T}^H\\ \mathbf{T} & \mathbf{T}\mathbf{T}^H\end{bmatrix}\mathbf{P}^H\mathbf{B}^H\mathbf{F}_N\mathbf{e}^H(f) + P_{x,u}(f). \tag{16}$$

In [17], it is shown that the average energy for the redundant symbols is given by $\sigma^2 trace(\mathbf{T}\mathbf{T}^H) = \sigma^2 trace(\mathbf{T}^H\mathbf{T})$ (in this paper, we assume $\sigma^2 = 1$). Further, assuming that the number of redundant carriers equals the unique word length (which is the minimum possible number of redundant carriers), i.e., $N_r = N_u$, [17] shows that the optimal redundant carrier placement that minimizes the required redundant energy results in the requirement that the matrix product $\mathbf{T}\mathbf{T}^H$ is a scaled identity matrix $\mathbf{T}\mathbf{T}^H = (N_d/N_r)\sigma^2\mathbf{I}_{N_r}$, and the resulting total energy of the redundant carriers equals the total energy of the data symbols, i.e., $\sigma^2 N_d$. Hence, the optimal redundant carrier placement evenly spreads the redundant energy over the different redundant carriers, with as a result an energy per redundant carrier equal to $(N_d/N_r)\sigma^2$. Taking into account that $\mathbf{P}$ is a permuted identity matrix to select the data carriers and redundant carriers, the level of $P_{x,d}(f)$ at carrier frequencies m/NT_s will be σ^2 for a data carrier and $(N_d/N_r)\sigma^2$ for a redundant carrier. In practice, to have a high throughput efficiency, the number of redundant carriers should be small as compared to the number of data symbols, so that $N_r/N_d << 1$. Taking into account that the energy per redundant carrier equals $(N_d/N_r)\sigma^2$, this energy will be much higher than the energy transmitted on a data carrier, σ^2. Hence, the in-band of $P_{x,d}(f)$ will show a strong ripple, with peaks at the redundant carrier positions.

B. Spectral Analysis of the Non-Systematic Coded UW-OFDM

For the case of the non-systematic coded UW-OFDM, we use the proposed simple code generator matrix design (7). To evaluate the behavior of $P_{x,d}(f)$ in the in-band, we take a closer look at the diagonal elements of $\mathbf{B}\mathbf{G}\mathbf{G}^H\mathbf{B}^H = \mathbf{B}\mathbf{N}_Q\mathbf{C}\mathbf{C}^H\mathbf{N}_Q^H\mathbf{B}^H$. In the case where $N_r = N_u$, $\mathbf{C}$ is a square matrix that can be selected freely. However, to minimize the MSE of the BLUE and LMMSE equalizers, $\mathbf{C}$ must satisfy $\mathbf{C}^H\mathbf{C} = \mathbf{I}$. As $\mathbf{C}$ is a square matrix, this also implies $\mathbf{C}\mathbf{C}^H = \mathbf{I}$, so that the in-band behavior becomes independent of the selected matrix $\mathbf{C}$, but only depends on the diagonal elements of the matrix $\mathbf{B}\mathbf{N}_Q\mathbf{N}_Q^H\mathbf{B}^H$. In Fig. 3, the diagonal elements are illustrated assuming the non-modulated carriers are located at the DC carrier and at the edges of the frequency band. As can be observed, on the modulated carrier positions, i.e. in the in-band, the diagonal elements are relatively constant: they only show a small ripple around the level N_d/N_{dr}.

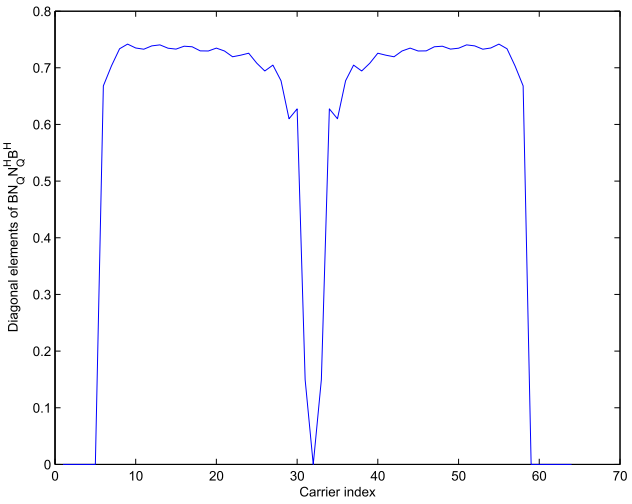

Fig. 3. Diagonal elements of $\mathbf{B}\mathbf{N}_Q\mathbf{N}_Q^H\mathbf{B}^H$ for $N_r = N_u = 16$, $N = 64$ and $N_z = 12$ (DC carrier and 11 band edge carriers).

TABLE I
MAIN PHY PARAMETERS OF THE INVESTIGATED SYSTEMS

	CP-OFDM	UW-OFDM
Number of subcarriers	64	$N = 64$
Occupied subcarriers	52	$N_{dr} = 52$
Data subcarriers	48	$N_d = 36$
zero subcarriers	12	$N_z = 12$
Additional subcarriers	4 (pilots)	$N_u = 16$ (UW)
DFT period	3.2 μs	3.2 μs
Guard duration	800 ns	800 ns
Total OFDM symbol duration	4 μs	3.2 μs
Bandwidth	20 MHz	20 MHz
Modulation scheme	16QAM	16QAM

Only the diagonal elements corresponding to the modulated carriers next to the non-modulated carriers show a sharp drop. Hence, in contrast to systematic coded UW-OFDM, in non-systematic UW-OFDM, the PSD corresponding to the data part will be relatively flat. Taking into account that $\mathbf{N}_Q^H\mathbf{B}^H\mathbf{B}\mathbf{N}_Q = \mathbf{I}_{N_d}$, and therefore $trace\{\mathbf{N}_Q^H\mathbf{B}^H\mathbf{B}\mathbf{N}_Q = \mathbf{I}_{Nd}\} = N_d = trace\{\mathbf{B}\mathbf{N}_Q\mathbf{N}_Q^H\mathbf{B}^H\}$, it follows that the energy in non-systematic UW-OFDM is more or less evenly spread over the N_{dr} modulated carriers.

IV. Simulation Results and Spectrum Analysis

In this section, simulation results are provided to examine the accuracy of the proposed analytical expressions for the PSD of the UW-OFDM system, and the UW-OFDM PSD is compared with the PSD of the conventional CP-OFDM system.[2] Also, the effect of the different parameters of the UW-OFDM transmitter on the PSD and especially on the OOB is investigated. In the literature (as e.g. [4], [5]), the UW-OFDM system performance is compared to that of the CP-OFDM system based on the IEEE 802.11a WLAN standard, therefore, we consider the system parameters as in Table I [28]. The indices of the $N_z = 12$ zero subcarriers for both CP-OFDM and UW-OFDM systems are $\{0, 27, 28, \ldots, 37\}$. Without loss of generality, it is assumed that $N_r = N_u$. For plotting the simulated PSDs, 5000 independent OFDM symbols are randomly generated, and Welch's periodogram algorithm is used to calculate the PSD of the transmitted signals. To allow a fair comparison, the energy per bit is considered to be the same for all simulated multicarrier systems.

[2]To gain more insight in the results, the analytical expression for the PSD of CP-OFDM is presented in Appendix B.

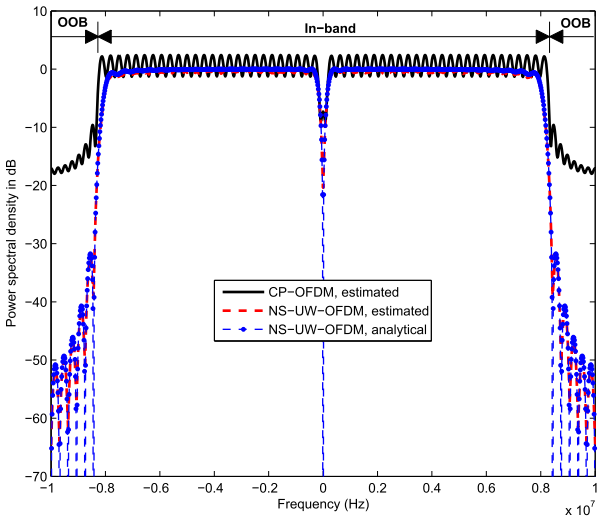

Fig. 4. PSD of non-systematic coded UW-OFDM compared to the PSD of CP-OFDM.

A. Accuracy of the Derived Analytical Expressions

In Fig. 4, the analytical expression for the PSD of the non-systematic coded (NS-) UW-OFDM signal, before adding the UW and without low-pass filtering, i.e. $P_{x,d}(f)$, is compared to the estimated PSD obtained from the simulations, and also to the estimated PSD of the IEEE 802.11a WLAN CP-OFDM signal before the interpolation filter. The analytically derived PSD curve fully matches the estimated curve. As mentioned in section III-B, the non-systematic UW-OFDM PSD is essentially flat in the in-band, which is occupied by the coded data, whereas the CP-OFDM PSD shows ripples that are introduced by the cyclic prefix. In the out-of-band, e.g. at frequency $1/T_s = 10$ MHz, the OOB radiation of the UW-OFDM is about -50 dB, which is drastically lower than the -20 dB OOB radiation of the CP-OFDM system.

In Fig. 5, the results are shown for systematic-coded UW-OFDM (S-UW-OFDM). Again, the analytical results are very close to the estimated PSD curve for both the in-band and out-of-band. The figure clearly shows the ripple in the in-band caused by the high redundant energy (see Section III-A). Comparing Figs. 4 and 5, the out-of-band radiation of NS-UW-OFDM and S-UW-OFDM are the same. So, (both types of) UW-OFDM systems exhibit the same interestingly low sidelobes. This makes them very useful for dynamic spectrum access (cognitive radio) applications where the transmitter uses vacant parts of the spectrum while not interfering with adjacent bands used by other legacy users.[3]

[3]For all investigated cases, simulations show that the theoretical results are in complete agreement with the simulated PSDs. Hence, for the sake of clarity of the figures, in the remainder of paper, we will show the analytical results only. Further, as the effect of the system parameters on both UW-OFDM types turns out to be the same, we restrict our attention to the NS-UW-OFDM case.

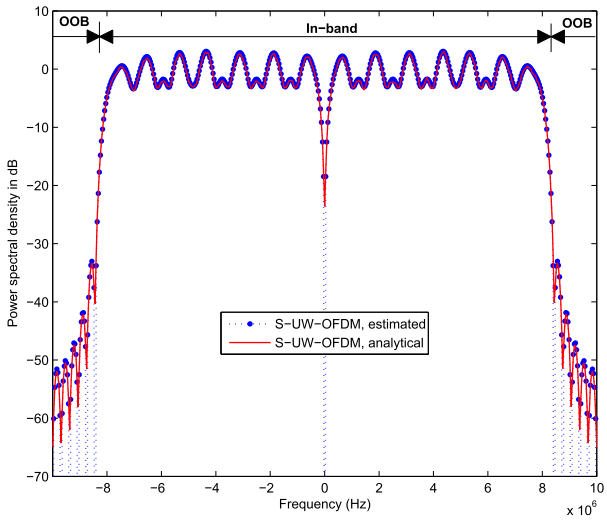

Fig. 5. PSD of systematic coded UW-OFDM for different redundant carrier placement approaches.

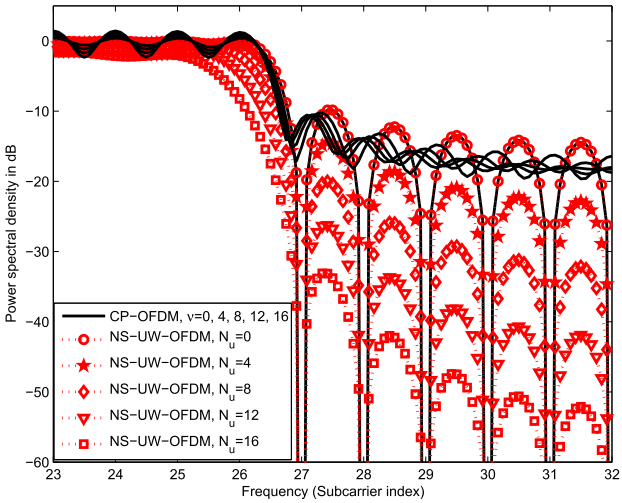

Fig. 6. Effect of N_u/N on OOB radiation of non-systematic coded UW-OFDM (dotted lines with different markers) compared to the the effect of ν/N on OOB radiation of CP-OFDM (solid lines).

B. Effect of System Parameters on OOB Radiation

We have found through numerical evaluation that the OOB radiation of UW-OFDM is a function of two parameters: the ratio N_u/N of the UW length to the number of subcarriers and the guard band length γ where $N_z = 2\gamma$ (this includes the zero DC subcarrier). To compare the results, we characterize the OOB radiation by two parameters: the first parameter is the roll-off factor (β), which is measured as the level of the first strongest peak in the OOB, and is an indication of the steepness of the PSD in the OOB. The second parameter is the OOB radiation level at the edge subcarriers (α). In the following figures, the effect of the system parameters on the OOB radiation characteristics is discussed.

First, we consider the effect of N_u/N on the OOB radiation. In Fig. 6, the PSD of the UW-OFDM is shown for different values of N_u (and thus for different N_u/N), assuming $\gamma = 6$ carriers at the edge of the frequency band are not used. For CP-OFDM, the counterpart of UW is the cyclic prefix ν; therefore, in the figure, we also show the PSD of CP-OFDM with the same cyclic prefix lengths as the UW: $\nu = N_u$. Note that the PSD of UW-OFDM with $N_u = 0$ coincides with that of CP-OFDM with zero cyclic prefix length: these two systems are identical. In the figure, we observe that when the CP length increases, it will only have a marginal effect on the level of the OOB radiation (α) and the roll-off (β), whereas in the in-band, it causes an increase of the ripples. This can be explained as follows. Typically, discrete-time implemented OFDM symbols in the time-domain are generated by a rectangular window. Therefore, the PSD of CP-OFDM can be modeled as the sum of periodic sinc-functions [1]. The power of sidelobes of the sinc-functions decays slowly as f^{-2}, where f is the distance in frequency to the main lobe [23]. By increasing the CP length, the sinc-functions will become narrower as the time-domain window length increases. However, as the sampling frequency does not change, the carrier frequency positions do not change fundamentally. Hence, the only noticeable effect will be a larger ripple due to the narrower main lobe. On the other hand, for UW-OFDM, Fig. 6 shows that increasing N_u results in an increase of the roll-off factor as well as a reduction of the OOB radiation level at the edge carriers. Both the roll-off factor and the level of the OOB radiation, expressed in dB, are shifted down in a linear way when N_u increases. To have more insight in the effect of increasing N_u on α and β, the values of these parameters are enumerated in Table II based on Fig. 6 together with the average transmission power in the in-band. It is seen that by increasing N_u by four, the roll-off factor (β) increases by about 6 dB and the OOB radiation at the edge carriers (α) increases by about 10 dB, while the average transmitted power in the in-band only slightly reduces with 0.3 dB. However, because of the complex analytical relationship between the system parameters and the matrices $\mathbf{T}$ and $\mathbf{G}$, no analytical explanation for the behavior at the OOB radiation as function of N_u could be found.

TABLE II
THE EFFECT OF N_u ON THE ROLL-OFF FACTOR (β) AND THE OOB RADIATION (α) AT THE EDGE CARRIERS

UW length (N_u)	0	4	8	12	16
In-band average power in dB	0	-0.3	-0.6	-1	-1.3
roll-off factor (β) in dB	-10	-14.5	-20	-26	-33
OOB at the edge carriers (α) in dB	-14.5	-23	-32	-42	-52

The second parameter that influences the OOB radiation of the UW-OFDM system is the width of the guard band, γ. In Fig. 7, this is illustrated for $N_u/N = 0.25$. Increasing the guard band length in UW-OFDM will strongly reduce both the roll-off (β) and the level of the OOB radiation (α), whereas in CP-OFDM, the effect of increasing γ is marginal. Again this can be explained by the fact that in UW-OFDM, changing γ will result in a change in the matrix $\mathbf{G}$ or $\mathbf{T}$, whereas in CP-OFDM, the only effect of increasing γ is that more sinc-functions are deactivated, which in fact will not dramatically change the spectral behavior of the sum of the remaining active sinc-functions. In Fig. 7, we observe that for UW-OFDM, both the roll-off factor and the level of the OOB radiation at the edge carriers (expressed in dB) will decrease linearly

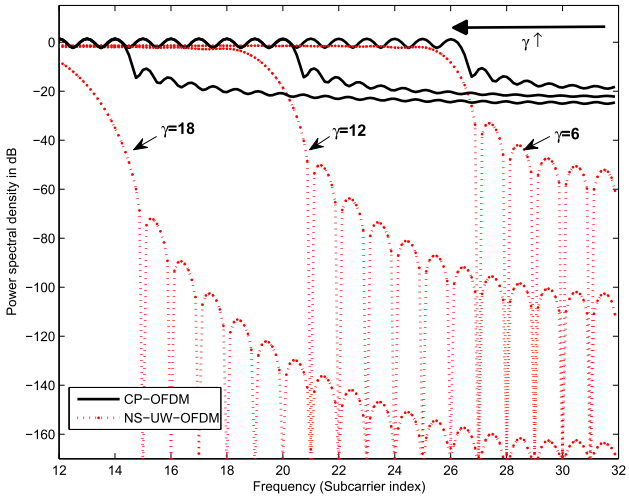

Fig. 7. Effect of γ on OOB radiation of non-systematic coded UW-OFDM (dotted lines) and CP-OFDM (solid lines) for $\gamma = 6, 12, 18$.

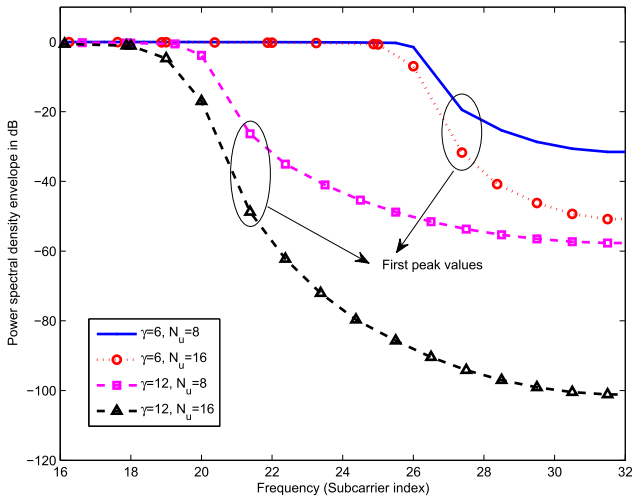

Fig. 8. Comparing the effect of guard band width γ and the unique word length N_u on the OOB radiation of non-systematic coded UW-OFDM.

with increasing γ, and reaches a lower limit of -160 dB for $\gamma = 18$, which is essentially zero. Again, the complex expressions for $\mathbf{T}$ and $\mathbf{G}$ obstructed the derivation of simple analytical expressions to explain the effect of γ.

In the previous results, we showed that increasing both the UW length N_u and the guard band width γ have a beneficial effect on the OOB radiation. We compare the effect of N_u and γ in Fig. 8. Consider the curve ($\gamma = 6$, $N_u = 8$) as the reference curve. Comparing the curves ($\gamma = 6$, $N_u = 16$) and ($\gamma = 12$, $N_u = 8$), where the number of guard subcarriers and the unique word length are doubled respectively, it is seen that for the first case ($\gamma = 6$, $N_u = 16$), the roll-off factor (β) is larger, whereas for the second case ($\gamma = 12$, $N_u = 8$), the level of the OOB radiation at the edge carriers (α) is lower. Hence, the UW length can be used to improve the roll-off factor, and the guard band width, γ, to lower the OOB radiation level at the edge carriers. Moreover, increasing both parameters (the case ($\gamma = 12$, $N_u = 16$)) improves the OOB radiation tremendously, but at the expense of reduced bandwidth efficiency.

Note that the functionality of the two parameters is different. The guard band carriers are introduced in the frequency domain, and are solely intended to suppress the OOB radiation. On the other hand, the UW sequence is inserted in the time domain, and its main functionality is that of the cyclic prefix in CP-OFDM: to control the frequency selectivity of the channel. This implies that its length N_u is mainly determined by the channel. This will set a lower bound on N_u, but in theory, we could increase the UW length. Of course, increasing N_u will reduce the data throughput, but this remark also holds for an increase of γ: the number of data symbols that can be transmitted (assuming $N_r = N_u$) equals $N_d = N - N_u - 2\gamma$. Hence, increasing γ will decrease the data throughput twice as fast as increasing N_u with the same amount. In practice, a compromise between the data throughput and the reduction of the OOB radiation by increasing N_u and γ must be found.

C. Effect of Unique Word and Low Pass Filter on the Spectrum

Until now, we have analyzed the OOB radiation of UW-OFDM in case of a zero unique word and before D/A conversion. However, these aspects will also play an important role in the overall spectrum. Hence, in this section, we look at how these two aspects will influence the good OOB radiation properties of UW-OFDM.

Let us first look at the effect of the unique word. To have a fair comparison to the CP-OFDM system used in the IEEE 802.11a standard, the energy of the unique word sequence related to the total mean energy of the UW-OFDM block is considered to be $4/52$. A sequence that is often used for channel estimation and synchronization[4] is the CAZAC (constant amplitude, zero autocorrelation) sequence [29]. In Fig. 9, the effect of the CAZAC sequence on the spectrum of UW-OFDM (before D/A conversion) is shown. The power spectrum, $P_{x,u}(f)$, of the CAZAC sequence is spread over all frequencies, and adding this CAZAC sequence to the data part results in the overall spectrum, $P_x(f)$. It can be observed that the CAZAC sequence will not considerably alter the in-band part of the spectrum, because the power of the unique word is low as compared to the energy assigned to the data symbols. However, the OOB radiation is dominated by the CAZAC UW energy, as at these frequencies, the contribution of the data part, i.e. $P_{x,d}(f)$, is very low (see Figs. 4 and 5). Hence, the presence of the CAZAC unique word degrades the good OOB performance of UW-OFDM. This motivated us to look for unique word sequences that preserve the good OOB performance of UW-OFDM.

A good UW sequence (in the context of the OOB radiation) should have a small amplitude at the higher out-of-band frequencies. Here, we propose a simple approach to design such a UW, based on the null space approach proposed in Section II-B for the data part. Similar to the data contribution, the unique word contribution can be written as a $N \times 1$ time domain vector. However, in contrast to the data part, which

[4]As the unique word is a known sequence, it can be used for channel estimation and synchronization.

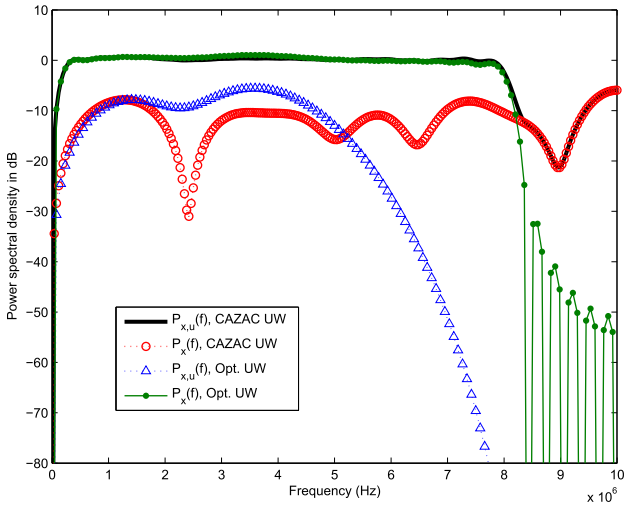

Fig. 9. Effect of the different unique words on the PSD of UW-OFDM.

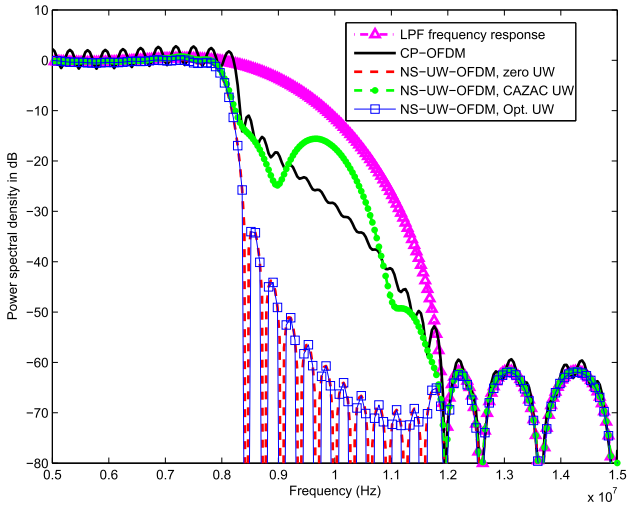

Fig. 10. Effect of interpolation low pass filter on the PSD of UW-OFDM.

must contain zeros at the last N_u positions, the unique word must have zeros at the first $N - N_u$ positions. Let us consider the frequency domain equivalent of this unique word, using the same structure as the data contribution:

$$\mathbf{x}'_u = \begin{bmatrix} \mathbf{0}_{(N-N_u)\times 1} \\ \mathbf{x}_u \end{bmatrix} = \mathbf{F}_N^H \mathbf{B} \mathbf{J} \tilde{\mathbf{x}}_u,$$

where $\mathbf{J}$ is a matrix similar to the code generator matrix, $\mathbf{G}$, which should be selected to generate the zeros in the first $(N - N_u)$ rows at the output of the IDFT. By using the same null space approach proposed in Section II-B, $\mathbf{J}$ is selected to be in the null space of the first $(N - N_u)$ rows of $\mathbf{F}_N^H \mathbf{B}$. Assuming $N - N_u < N - N_z$, $N_u - N_z$ linearly independent null space vectors exist, which are stacked to construct the $(N-N_z)\times(N_u-N_z)$ matrix $\mathbf{J}$. The $(N_u-N_z)\times 1$ vector $\tilde{\mathbf{x}}_u$ can be selected freely. This choice of the unique word guarantees that the first $(N - N_u)$ samples of the unique word vector $\mathbf{x}'_u$ are zero. Note that the proposed approach for designing the unique word is applicable for the cases where $N_u \geq N_z$.

The power spectra of of $P_{x,u}(f)$ and $P_x(f)$ for this optimized unique word are also depicted in Fig. 9. Similarly as the data part, the optimized unique word has very small values in the OOB. Hence, it is possible to keep the good OOB radiation properties of UW-OFDM, even when the unique word is added.

Next, we look at the effect of the D/A conversion on the spectrum. As stated in Section III, since the UW-OFDM is generated in the discrete-time domain, its spectrum is periodic with period $1/T_s$. The interpolation filter at the output of the D/A has as main responsibility the suppression of the OOB radiation of the multicarrier system, including the periodic contribution. The analytical PSD, $P(f)$, for UW-OFDM is obtained from (9) by multiplying the frequency response of the interpolation filter with $P_x(f)$. A zoomed plot of the OOB radiation is shown in Fig. 10 for CP-OFDM, and the NS-UW-OFDM system with a zero, a CAZAC and an OOB-optimized unique word. The interpolation filter used in this figure is a 22nd-order equiripple, finite impulse response filter with 60 dB stopband attenuation and a passband ripple of 1 dB. It can be seen that for the zero UW and the optimized UW, the high roll-off factor of the UW-OFDM spectrum combined with the OOB reduction ability of the lowpass filter results in a very sharp drop in the OOB. For conventional CP-OFDM, the OOB roll-off factor is much lower. The roll-off factor of UW-OFDM with a non-optimized CAZAC UW is at the same level of CP-OFDM.

V. Conclusion

In this paper, the characterization of the PSD of UW-OFDM is addressed. In this system, the insertion of redundancy in the frequency domain creates correlation in the UW-OFDM block. So, the conventional spectral modeling approaches for CP-OFDM that assume the independency of the frequency domain data vectors are not applicable to UW-OFDM systems. However, the correlation pattern is repeated each UW-OFDM block making the time domain data sequence to be cyclostationary. The PSD is derived by calculating the Fourier transform of an OFDM block and statistically averaging squared magnitude of the resulting frequency domain samples over all UW-OFDM blocks. The simulation results have shown the accuracy of the derived expression. A first conclusion is that the OOB radiation is much lower than for CP-OFDM. Further, we show that two system parameters have a large influence on the OOB radiation of UW-OFDM, i.e. the unique word length N_u, and the guard band width γ. The first parameter, N_u, is well suited to increase the roll-off of the OOB radiation, whereas the second parameter γ has a large influence on the level of the radiation at the edge carriers. Further, we show in this paper that if the unique word is not properly designed, the good OOB radiation properties of UW-OFDM are lost. In this paper, we propose a construction method for the unique word to keep the excellent OOB radiation properties.

Appendix

A. The length of the Data Segments

Consider the block based representation of the UW-OFDM signal in (10). Without loss of generality, let us consider each segment contains L UW-OFDM blocks. The DTFT of one of

the segments covering the UW-OFDM blocks with the indices $\{l_1, l_1+1, \ldots, l_1+L-1\}$ can be written as

$$X^{(l_1,L)}(f) = \frac{1}{\sqrt{LN}} \sum_{l=l_1}^{l_1+L-1} \sum_{n=0}^{N-1} x_n^{(l)} e^{-j2\pi\alpha f T_s}, \quad (17)$$

where $\alpha = n + (l-l_1)N$. To estimate the PSD in Bartlett's method, the squared magnitude of the DTFT of the different data segments are time-averaged. The modulated data symbols in the frequency domain are assumed to be i.i.d.. So, after being modulated by the UW-OFDM transmitter, the data sequence in the time domain data sequence becomes cyclostationary [1], [25]. As the statistical properties of the UW-OFDM signal are known, we replace the time-averaging with the statistical expectation. Therefore, we have

$$\begin{aligned} P_x(f) &= E\left[\left|X^{(l_1,L)}(f)\right|^2\right] \\ &= \frac{1}{LN} E\Bigg[\left(\sum_{l=l_1}^{l_1+L-1} \sum_{n=0}^{N-1} x_n^{(l)} e^{-j2\pi\alpha f T_s}\right) \\ &\quad \cdot \left(\sum_{l'=l_1}^{l_1+L-1} \sum_{n'=0}^{N-1} x_{n'}^{(l')*} e^{+j2\pi\beta f T_s}\right)\Bigg] \end{aligned} \quad (18)$$

where $\beta = n' + (l'-l_1)N$. As data symbols in different blocks are independent, we have

$$\begin{aligned} P_x(f) &= \frac{1}{LN} \sum_{l=l_1}^{l_1+L-1} E\left[\left(\sum_{n=0}^{N-1} \sum_{n'=0}^{N-1} x_n^{(l)} x_{n'}^{(l)*} e^{-j2\pi(n-n')f T_s}\right)\right] \\ &= E\left[\left|X^{(l)}(f)\right|^2\right]. \end{aligned} \quad (19)$$

B. The PSD Expression for CP-OFDM

Suppose $\mathbf{d} = [d_1, d_2, \ldots, d_{\tilde{N}_d}]$ is the $\tilde{N}_d \times 1$ data vector to be transmitted by CP-OFDM. The frequency domain data vector is given as $\mathbf{x} = \mathbf{B}\mathbf{d}$, where $\mathbf{B} \in \mathbb{R}^{N\times(N-\tilde{N}_d)}$ inserts the zero carriers. This frequency domain data is converted to time-domain and preceded by the cyclic prefix with the length ν. The time-domain data vector is given by

$$\mathbf{s} = \mathbf{W}^H \mathbf{D}\mathbf{B}\mathbf{d}. \quad (20)$$

where $\mathbf{W} \in \mathbb{C}^{M\times N}$ is a Fourier matrix with the (m,n)th entry $[\mathbf{W}]_{m,n} = \frac{1}{\sqrt{N}} e^{-j2\pi mn/N}$, $M = N+\nu$, and $\mathbf{D} = diag([1, e^{-j2\pi\nu/N}, \ldots, e^{-j2\pi\nu(N-1)/N}]$ is a $N \times N$ diagonal matrix, modeling the CP addition. Following the same procedure as in Sec. III, the PSD of the discrete-time CP-OFDM data sequence before the interpolation filter can be expressed as

$$P_s^{CP}(f) = \tilde{\mathbf{e}}(f)\mathbf{W}^H\mathbf{D}\mathbf{B}\mathbf{B}^H\mathbf{D}^H\mathbf{W}\tilde{\mathbf{e}}^H(f) \quad (21)$$

where $\tilde{\mathbf{e}}(f)$ is a $1 \times M$ row vector with as mth entry $e^{-j2\pi mfT_s}/\sqrt{N}$.

ACKNOWLEDGMENT

The work that led to this paper was done during the visit of Morteza Rajabzadeh at the Department of Telecommunications and Information Processing, Ghent University.

REFERENCES

[1] T. van Waterschoot, V. Le Nir, J. Duplicy, and M. Moonen, "Analytical expressions for the power spectral density of CP-OFDM and ZP-OFDM signals," *IEEE Signal Process. Lett.*, vol. 17, no. 4, pp. 371–374, Apr. 2010.

[2] H. Steendam and M. Moeneclaey, "Different guard interval techniques for OFDM: Performance comparison," in *Multi-Carrier Spread Spectrum*. Basel, Switzerland: Springer, 2007, pp. 11–24.

[3] S. Tang, F. Yang, K. Peng, C. Pan, K. Gong, and Z. Yang, "Iterative channel estimation for block transmission with known symbol padding—A new look at TDS-OFDM," in *Proc. IEEE Global Telecommun. Conf. (GLOBECOM)*, Nov. 2007, pp. 4269–4273.

[4] A. Onic and M. Huemer, "Direct vs. two-step approach for unique word generation in UW-OFDM," in *Proc. 15th Int. OFDM Workshop*, 2010, pp. 285–299.

[5] M. Huemer, C. Hofbauer, and J. B. Huber, "Non-systematic complex number RS coded OFDM by unique word prefix," *IEEE Trans. Signal Process.*, vol. 60, no. 1, pp. 285–299, Jan. 2012.

[6] C. Hofbauer, M. Huemer, and J. B. Huber, "On the impact of redundant subcarrier energy optimization in UW-OFDM," in *Proc. 4th Int. Conf. Signal Process. Commun. Syst. (ICSPCS)*, Dec. 2010, pp. 1–6.

[7] C. Hofbauer and M. Huemer, "A study of data rate equivalent UW-OFDM and CP-OFDM concepts," in *Proc. IEEE ASILOMAR*, Nov. 2012, pp. 173–177.

[8] M. Huemer, C. Hofbauer, A. Onic, and J. B. Huber, "On the exploitation of the redundant energy in UW-OFDM: LMMSE versus sphere detection," *IEEE Signal Process. Lett.*, vol. 19, no. 6, pp. 340–343, Jun. 2012.

[9] C. Hofbauer, M. Huemer, and J. B. Huber, "Coded OFDM by unique word prefix," in *Proc. IEEE Int. Conf. Commun. Syst. (ICCS)*, Nov. 2010, pp. 426–430.

[10] M. Huemer, A. Onic, and C. Hofbauer, "Classical and Bayesian linear data estimators for unique word OFDM," *IEEE Trans. Signal Process.*, vol. 59, no. 12, pp. 6073–6085, Dec. 2011.

[11] A. Onic and M. Huemer, "Noise interpolation for unique word OFDM," *IEEE Signal Process. Lett.*, vol. 21, no. 7, pp. 814–818, Jul. 2014.

[12] H. Steendam, "Theoretical performance evaluation and optimization of UW-OFDM," *IEEE Trans. Commun.*, vol. 64, no. 4, pp. 1739–1750, Apr. 2016.

[13] M. Rajabzadeh, H. Steendam, and H. Khoshbin, "Power spectrum characterization of systematic coded UW-OFDM systems," in *Proc. IEEE 78th Veh. Technol. Conf. (VTC Fall)*, Sep. 2013, pp. 1–5.

[14] D. Chen, X.-G. Xia, T. Jiang, and X. Gao, "Properties and power spectral densities of CP based OQAM-OFDM systems," *IEEE Trans. Signal Process.*, vol. 63, no. 14, pp. 3561–3575, Jul. 2015.

[15] D. Chen, D. Qu, T. Jiang, and Y. He, "Prototype filter optimization to minimize stopband energy with NPR constraint for filter bank multicarrier modulation systems," *IEEE Trans. Signal Process.*, vol. 61, no. 1, pp. 159–169, Jan. 2013.

[16] H. Steendam, "Analysis of the redundant energy in UW-OFDM," *IEEE Trans. Commun.*, vol. 60, no. 6, pp. 1692–1701, Jun. 2012.

[17] H. Steendam, "On the selection of the redundant carrier positions in UW-OFDM," *IEEE Trans. Signal Process.*, vol. 61, no. 5, pp. 1112–1120, Mar. 2013.

[18] M. Rajabzadeh, H. Khoshbin, and H. Steendam, "Sidelobe suppression for non-systematic coded UW-OFDM in cognitive radio networks," in *Proc. 20th Eur. Wireless Conf.*, May 2014, pp. 1–6.

[19] C. Liu and F. Li, "Spectrum modelling of OFDM signals for WLAN," *Electron. Lett.*, vol. 40, no. 22, pp. 1431–1432, Oct. 2004.

[20] S. L. Talbot and B. Farhang-Boroujeny, "Spectral method of blind carrier tracking for OFDM," *IEEE Trans. Signal Process.*, vol. 56, no. 7, pp. 2706–2717, Jul. 2008.

[21] M. Pauli and P. Kuchenbecker, "On the reduction of the out-of-band radiation of OFDM-signals," in *Proc. IEEE Int. Conf. Commun.*, vol. 3. Jun. 1998, pp. 1304–1308.

[22] I. Cosovic, S. Brandes, and M. Schnell, "Subcarrier weighting: A method for sidelobe suppression in OFDM systems," *IEEE Commun. Lett.*, vol. 10, no. 6, pp. 444–446, Jun. 2006.

[23] J. A. Zhang, X. Huang, A. Cantoni, and Y. J. Guo, "Sidelobe suppression with orthogonal projection for multicarrier systems," *IEEE Trans. Commun.*, vol. 60, no. 2, pp. 589–599, Feb. 2012.

[24] Y.-P. Lin and S.-M. Phoong, "OFDM transmitters: Analog representation and DFT-based implementation," *IEEE Trans. Signal Process.*, vol. 51, no. 9, pp. 2450–2453, Sep. 2003.

[25] M. T. Ivrlač and J. A. Nossek, "Influence of a cyclic prefix on the spectral power density of cyclo-stationary random sequences," in *Multi-Carrier Spread Spectrum*. Basel, Switzerland: Springer, 2007, pp. 37–46.

[26] M. S. Babtlett, "Smoothing periodograms from time-series with continuous spectra," *Nature*, vol. 161, no. 4096, pp. 686–687, 1948.
[27] A. V. Oppenheim and R. W. Schafer, *Discrete-Time Signal Processing*, 3rd ed. Englewood Cliffs, NJ, USA: Prentice-Hall, 2010.
[28] *Wireless LAN Medium Access Control (MAC) and Physical Layer (PHY) Specifications: High-Speed Physical Layer in the 5 GHZ Band*, IEEE Standard 802.11a-1999(R2003), Sep. 1999.
[29] B. M. Popovic, "Generalized chirp-like polyphase sequences with optimum correlation properties," *IEEE Trans. Inf. Theory*, vol. 38, no. 4, pp. 1406–1409, Jul. 1992.

Morteza Rajabzadeh (M'14) received the B.Sc. and M.Sc. degrees (Hons.) in electrical engineering and the Ph.D. degree from the Ferdowsi University of Mashhad, Mashhad, Iran, in 2005, 2008, and 2014, respectively. From 2012 to 2013, he was a Visiting Scholar with the DIGCOM Group, TELIN Department, Ghent University. He is currently an Assistant Professor with the Quchan University of Technology, Quchan, Iran. His research interests include statistical signal processing, multicarrier techniques (especially CP-OFDM, MC-CDMA, and UW-OFDM), and cognitive radio networks.

Heidi Steendam (M'01–SM'06) received the M.Sc. degree in electrical engineering and the Ph.D. degree in applied sciences from Ghent University, Gent, Belgium, in 1995 and 2000, respectively. Since 1995, she has been with the Digital Communications Research Group, Department of Telecommunications and Information Processing, Faculty of Engineering, Ghent University, first in the framework of various research projects, and since 2002, as a full-time Professor in digital communications. She is the author of over 140 scientific papers in international journals and conference proceedings, for which several best paper awards were received. Her research interests include statistical communication theory, carrier and symbol synchronization, bandwidth-efficient modulation and coding, cognitive radio, and cooperative networks and positioning. Since 2002, she has been an Executive Committee Member of the IEEE Communications and Vehicular Technology Society Joint Chapter, Benelux Section, and since 2012, she has been the Vice Chair. She has been active in various international conferences as a Technical Program Committee Chair/Member and a Session Chair. In 2004 and 2011, she was the conference Chair of the IEEE Symposium on Communications and Vehicular Technology in the Benelux. She is an Associate Editor of the IEEE TRANSACTIONS ON COMMUNICATIONS, the *EURASIP Journal on Wireless Communications and Networking*, and the *Journal on Communications and Network*.